CONF-900809--1

IODINE AND NO_x BEHAVIOR IN THE DISSOLVER OFF-GAS AND IODOX SYSTEMS IN THE OAK RIDGE NATIONAL LABORATORY INTEGRATED EQUIPMENT TEST FACILITY*

CONF-900809--1

DE90 015160

J. F. Birdwell
Fuel Recycle Division
Post Office Box 2008
Oak Ridge National Laboratory†
Oak Ridge, Tennessee 37831

A paper for presentation
at the
21st DOE/NRC NUCLEAR AIR CLEANING CONFERENCE

August 13-16, 1990

San Diego, California

*Research sponsored by the Office of Facilities, Fuel Cycle, and Test Programs for the U.S. Department of Energy under Contract No. DE-AC05-84OR21400 with Martin Marietta Energy Systems, Inc., and the Power Reactor and Nuclear Fuel Development Corporation of Japan.

†Operated by Martin Marietta Energy Systems, Inc., for the U.S. Department of Energy.

IODINE AND NO_x BEHAVIOR IN THE DISSOLVER OFF-GAS AND IODOX SYSTEMS IN THE OAK RIDGE NATIONAL LABORATORY INTEGRATED EQUIPMENT TEST FACILITY

J. F. Birdwell, Fuel Recycle Division
Oak Ridge National Laboratory*
Oak Ridge, Tennessee 37831

Abstract

This paper describes the most recent in a series of experiments evaluating the behavior of iodine and NO_x in the Integrated Equipment Test (IET) Dissolver Off-Gas (DOG) System. This work was performed as part of a joint collaborative program between the U.S. Department of Energy and the Power and Nuclear Fuel Development Corporation of Japan.

The DOG system consists of two shell-and-tube heat exchangers in which water and nitric acid are removed from the dissolver off-gas by condensation, followed by a packed tower in which NOx is removed by absorption into a dilute nitric acid solution. The paper also describes the results of the operation of the Iodine Oxidation (IODOX) System. This system serves to remove iodine from the DOG system effluent by absorption into hyperazeotropic nitric acid.

Prior to the most recent experiments, three phases of testing were performed, one in the laboratory and two in the IET facility. Significant modifications in operational and experimental procedures were introduced during the latest test to simplify system operation and constituent analyses. These modifications included installing continuous NO_x analyzers, improving the control of air inleakage into the process, and using 131-I to facilitate iodine analysis by measuring the gamma activity level.

The results of the testing indicate strong and varied interactions between the components in the NO_x-H_2O-HNO_3 system. Due to the range of equilibrium relationships present in this system, the behavior of these components is strongly influenced by the relative concentration levels. The test results also indicate a reasonably high removal efficiency in the NO_x scrubber, even at relatively low feed gas concentrations.

Results from iodine testing indicate that only 2 to 4% of the iodine present in the vapor exiting the dissolver is returned to the dissolver in liquid recycle streams from the off-gas condensers and the NO_x scrubber. These results are consistent with those obtained in previous phases of testing. Some

---

*Operated by Martin Marietta Energy Systems, Inc., for the U.S. Department of Energy.

accumulation of iodine in the NO_x scrubber solution was observed. However, the short duration of the iodine test prevented the attainment of steady state in the scrubber with respect to iodine loading and distribution. Iodine removal efficiencies observed in the IODOX system were much lower than anticipated.

1. Background

The Integrated Equipment Test (IET) facility was constructed in the early 1980s as part of the Consolidated Fuel Reprocessing Program. The IET was built to provide a facility for the development and testing of processes and equipment used in the reprocessing of spent nuclear reactor fuel.

A principal chemical process in nuclear fuel reprocessing is the dissolution of the spent fuel, which consists of heavy metal oxides and various fission products. The process (which typically uses nitric acid as the dissolvent) results both in the formation of heavy metal nitrates and oxides of nitrogen (NO_x) and in the release of volatile fission products such as krypton, xenon, and iodine.

From its inception, the IET facility has utilized a continuous dissolution concept. This concept has been realized in the demonstration of a continuous rotary dissolver, which produces an aqueous uranyl nitrate/nitric acid solution when fed continuously with nitric acid and semicontinuously with uranium oxide. Associated with the dissolution process is an off-gas removal system for the treatment of the gaseous effluent. As originally installed, the DOG treatment system consisted of a packed NO_x scrubber and ancillary equipment (Fig. 1). This system serves the dual purposes of removing a large quantity of moisture from the DOG (which exits the dissolver at temperatures in the range 348 to 368 K) and reducing the DOG NO_x concentration to $\leq$ 1%. Both of these steps are prerequisites for effective removal of iodine in the IODOX process (Fig. 2) in which iodine is absorbed into hyperazeotropic nitric acid. Evaporation of the IODOX scrubber liquor results in the crystallization of hydroiodic acid (HI3O8) formed during absorption.

In facilities in which the heavy metal processing rate is relatively low (less than 0.5 tonne/day) the off-gas contribution from the dissolution reaction is small relative to the contributions from inleakage, instrument bubblers, and air spargers. As a result, the NO_x concentration in the DOG may be sufficiently low to have no adverse impact on the iodine removal efficiency of the IODOX process. In cases such as this, the only pretreatment required prior to iodine removal is drying.

Development of the double overhead condenser concept for DOG treatment was directed toward effectively cooling and drying the DOG while minimizing the amount of iodine recycled to the dissolver. Calculations performed using the equation for the

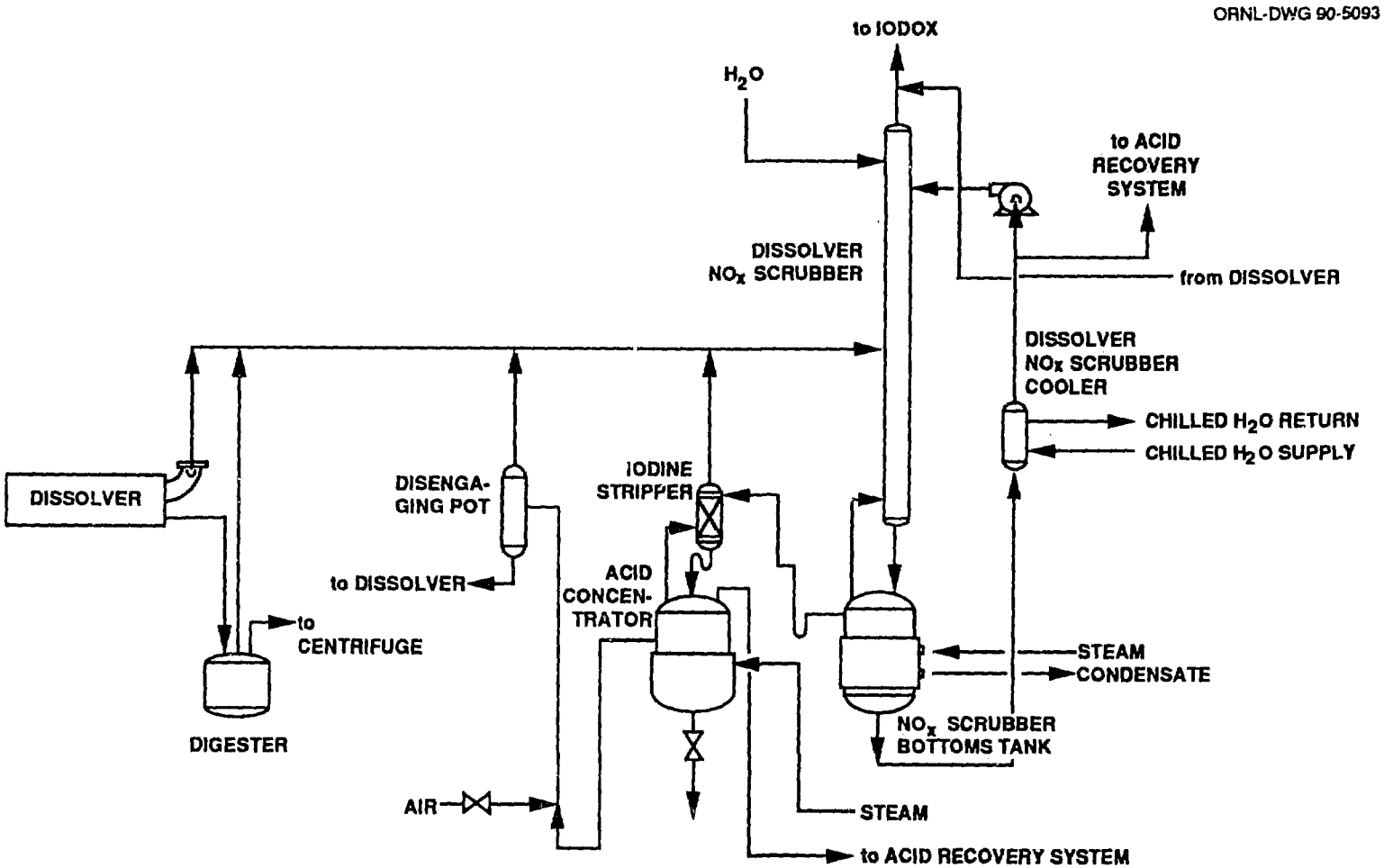

Fig. 1. Original configuration of IET dissolver, NO_x scrubber, and supporting equipment.

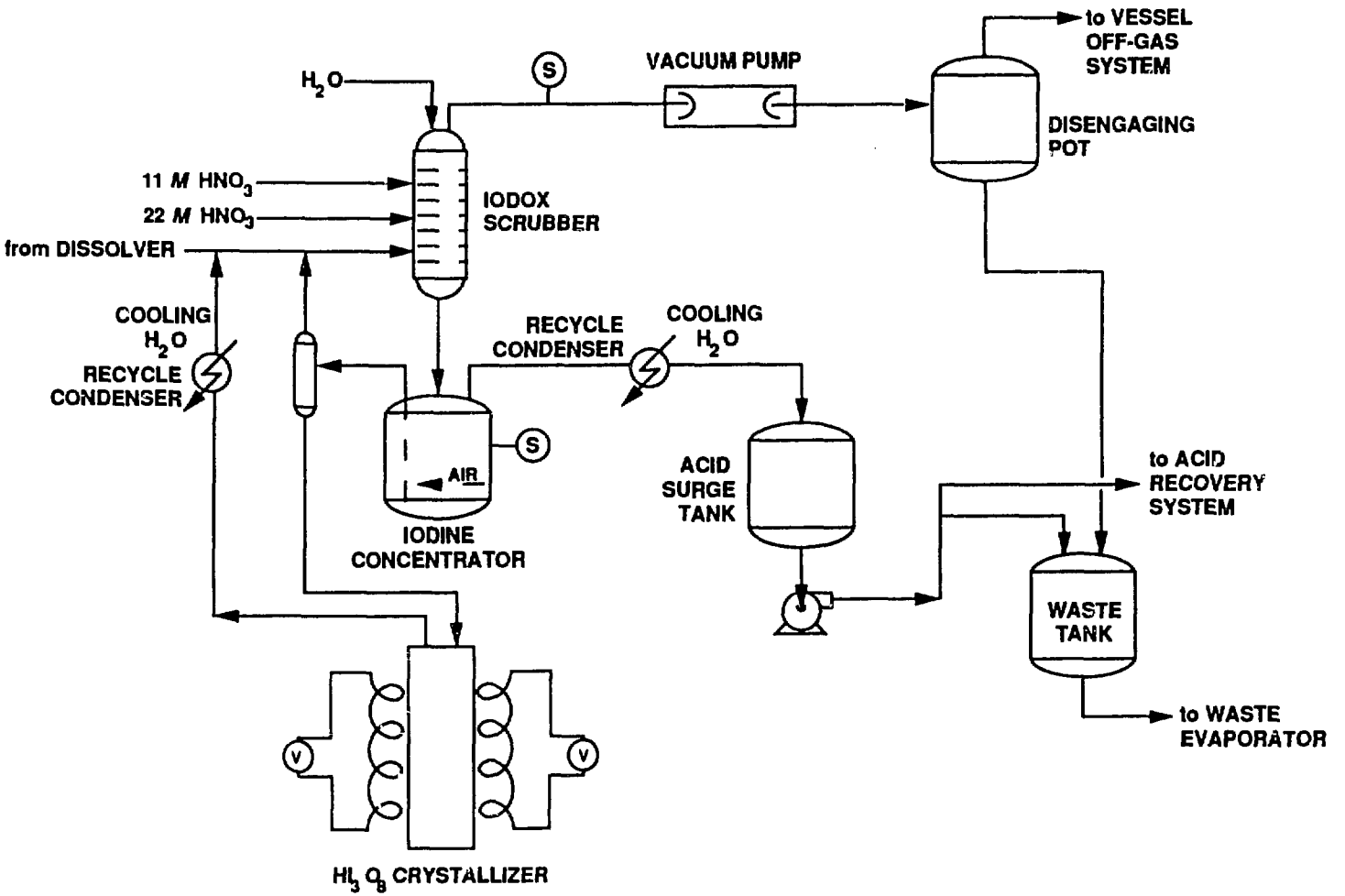

Fig. 2. IODOX system schematic with sample withdrawal points indicated.

iodine distribution coefficient,[1]

$$\ln D = [4793.4 - 150.9(M)](1/T) + 0.547(M) - 11.886 , \quad (1)$$

where

$D = I_2$ distribution coefficient, (molarity $I_2)_{liq}$/(molarity $I_2)_{gas}$,

T = temperature (K) ,

M = acid concentration in liquid (mol HNO_3/L) ,

indicated that a stepwise cooling of the DOG stream could accomplish these objectives. Based on these calculations, a laboratory evaluation of the viability of the double overhead condenser concept was performed. The results of this study provided qualitative confirmation that cooling and drying of the DOG could be achieved with excellent retention of the iodine in the vapor phase. Subsequently, two shell-and-tube condensers were installed in the IPD dissolver off-gas stream for testing (Fig. 3).[1] This testing was performed in two phases. In the first phase, the dissolver operating conditions were maintained within the normal temperature and pressure ranges without performing uranium oxide dissolution. Iodine was fed to the dissolver in the form of potassium iodide solution. In the second phase, the off-gas system was operated in conjunction with the shear, which delivered uranium oxide and simulated hulls to the dissolution system, generating NO_x.

Results from the first phase of experiments in the IPD indicate that the removal of iodine from the vapor phase is inversely proportional to temperature. This finding is consistent with Eq. (1), which yields increasing liquid/vapor distribution coefficients at decreasing temperatures. While the rate of gas flow did have some effect on the removal of iodine from the vapor phase, this relationship was not as pronounced as the correlation between temperature and liquid/vapor partitioning.

For the two condensers in series, the overall iodine removal efficiency was quite low, ranging from 0.35 to 6.29%. Individual removal efficiencies for the two condensers ranged from 0.03 to 5.78% for the first condenser and from 0.02 to 3.42% for the second condenser. In general, the results of this study indicated that the overall iodine removal efficiency was lowest when the first condenser operating temperature was in the 323 to 343 K temperature range.

The combined NO_x removal efficiency in the two condensers ranged from 5 to 58%, but was generally 20%, $\pm$7%. The overall NO_x efficiency for the DOG system (condensers and scrubber) ranged from 40 to 60%. Scrubber effluent NO_x concentrations ranged from 0.4 to 1.0%. Scrubber removal efficiencies were

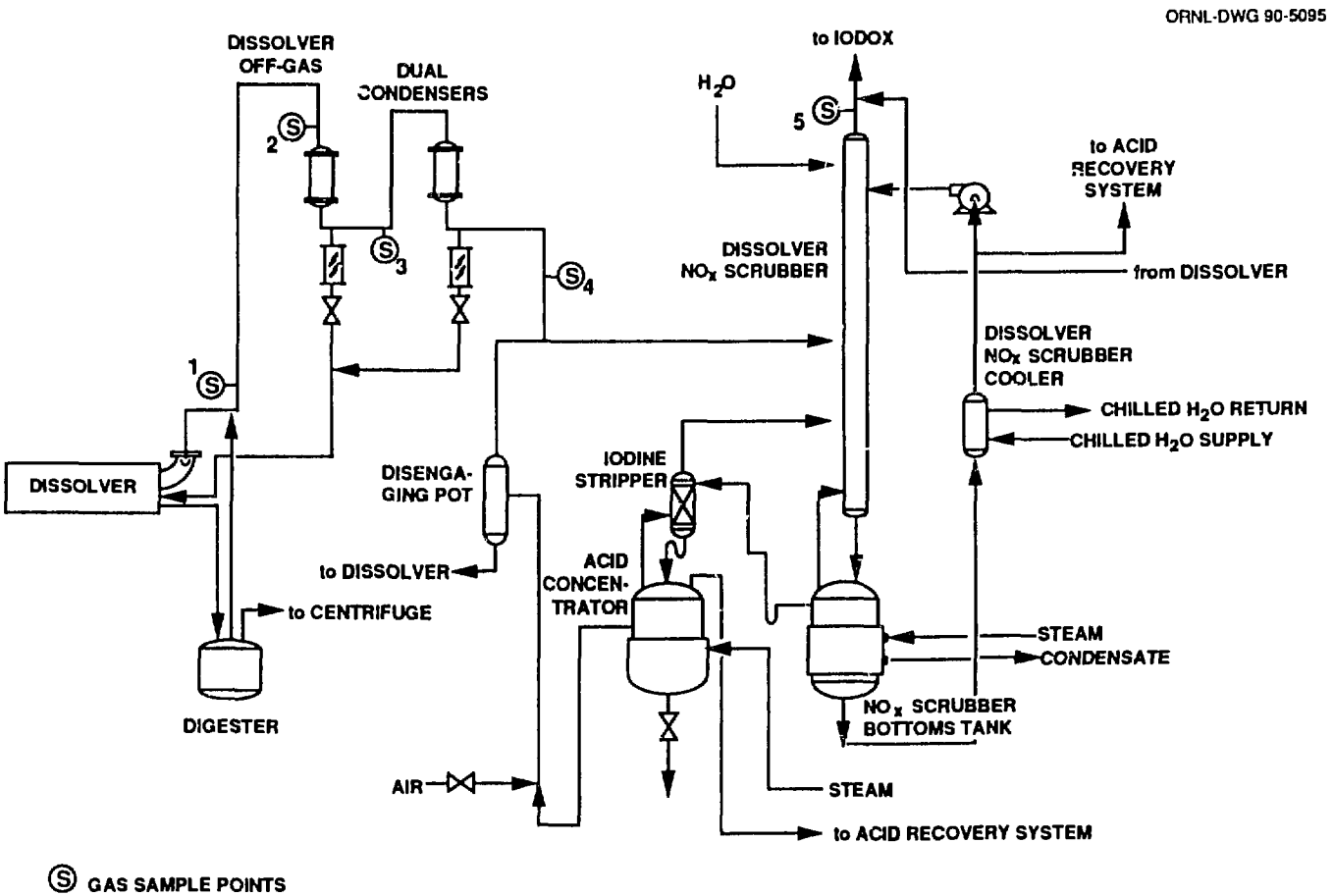

Fig. 3. Current configuration of IET dissolver and NO_x scrubbing system.

generally low because of low concentrations of NO_x present in the effluent from the second condenser.

It was observed that the NO_x removal efficiencies of the condensers and the scrubber complemented each other (i.e., under conditions at which scrubber efficiencies were low the condenser NO_x removal efficiencies were high. The results were the converse when scrubber efficiencies were high). In general, the observed NO_x removal capability of the condensers was greatest when the inlet NO_x concentration was low. This tendency suggested that the removal of NO_x in the condensers could be attributed primarily to the condensation of HNO_3, rather than the absorption of gaseous NO_x species into the liquid.

2. Objectives

The described testing provided useful information on the behaviors of iodine and NO_x in the DOG system. However, operational difficulties and limitations in the sampling and analytical techniques affected the precision and validity of the results. The more recent phases of testing were performed with modifications made in system operation, data collection, and analysis, which were intended to improve the quality of the data collected.

To minimize confusion between the two phases of experiments described in Sect. 1 and later work, the most recent off-gas experiments will be referred to as Phases 3 and 4. The primary objective of Phase 3 was to characterize the off-gas generated by the dissolution of uranium oxide. This test was performed by using the IET Feed Station to deliver feed material to the dissolver incrementally to simulate shear operation. In addition to determining the concentrations of nitrogen oxides in the DOG, gas- and liquid-phase samples were taken throughout the dissolver and DOG systems to obtain data regarding NO_x distribution and behavior in both phases.

The objectives of Phase 4 were (1) to study the behavior of NO_x and iodine in the off-gas system and (2) to evaluate the iodine and NO_x removal capabilities of the IODOX and DOG systems respectively. To both simplify system operation and provide the capability to vary test conditions, generating NO_x by dissolution of uranium oxide was replaced by feeding NO and NO_2 into the dissolver from gas cylinders. The gas feed rates were predetermined to produce NO_x concentrations in ranges approximating those observed in Phase 3 testing. Note that whereas dissolution of uranium oxide under simulated shear conditions generates off-gas in pulses, Phase 4 testing was performed at constant gas feed rates to simplify analysis of the results.

3. Description of Experiments

3.1 Phase 3

As stated in Sect. 2, Phase 3 off-gas was generated by introducing uranium oxide to the dissolver under conditions simulating feeding from a fuel shear device. Under these conditions, a feed increment consisting of uranium oxide and simulated sheared pin segments is fed to the dissolver once every 90 s. Based on an established shear operation scheme, complete shearing of one assembly requires 72 cuts. Therefore, the total duration of a dissolver feed period is 108 min. Again, based on assumed shear operating scenarios, a 72-min shear reload period was simulated during which no additional feed was introduced into the dissolver. Accordingly, a complete simulated shear cycle used in Phase 3 testing lasted 180 min.

NO_x samples were withdrawn at five locations throughout the DOG system: at the dissolver off-gas outlet (Sample Point 1), immediately upstream from the first condenser (Point 2), immediately upstream from the second condenser (Point 3), downstream from the second condenser (Point 4), and downstream from the DOG NO_x scrubbing column (Sample Point 5).

The results of Phases 1 and 2 indicated that moisture was condensing in the gas sample bombs as the samples were collected. Material balance calculations seemed to indicate that this condensation was resulting in the absorption of some NO_x from the sample prior to analysis. To mitigate this problem, a system of infrared NO and NO_2 analyzers was installed to provide online analysis capabilities. As shown in Figs. 4 and 5, the off-gas sample streams were drawn to the analyzers using vacuum pumps located downstream of each analyzer. Two analyzer stations were utilized, each consisting of one NO and one NO_2 analyzer. A valve panel was configured to allow switching between Sample Points 1, 2, and 3 at analyzer station A, and between Points 4 and 5 at analyzer station B. Before entering the analyzers, the gas sample streams from Points 1, 2, and 3 were passed through heat changers to cool and partially dry the gas, preventing condensate formation in the analyzers and the vacuum pumps. The off-gas conditions at Points 4 and 5 were such that additional drying was not required. The sample cells in the analyzers are maintained at a temperature of 328 K as further protection against condensate formation.

In addition to gas samples, liquid samples from the sample line condensers, overhead condensers, scrubber bottoms tank, and the acid concentrator were collected and analyzed for HNO_2 and HNO_3.

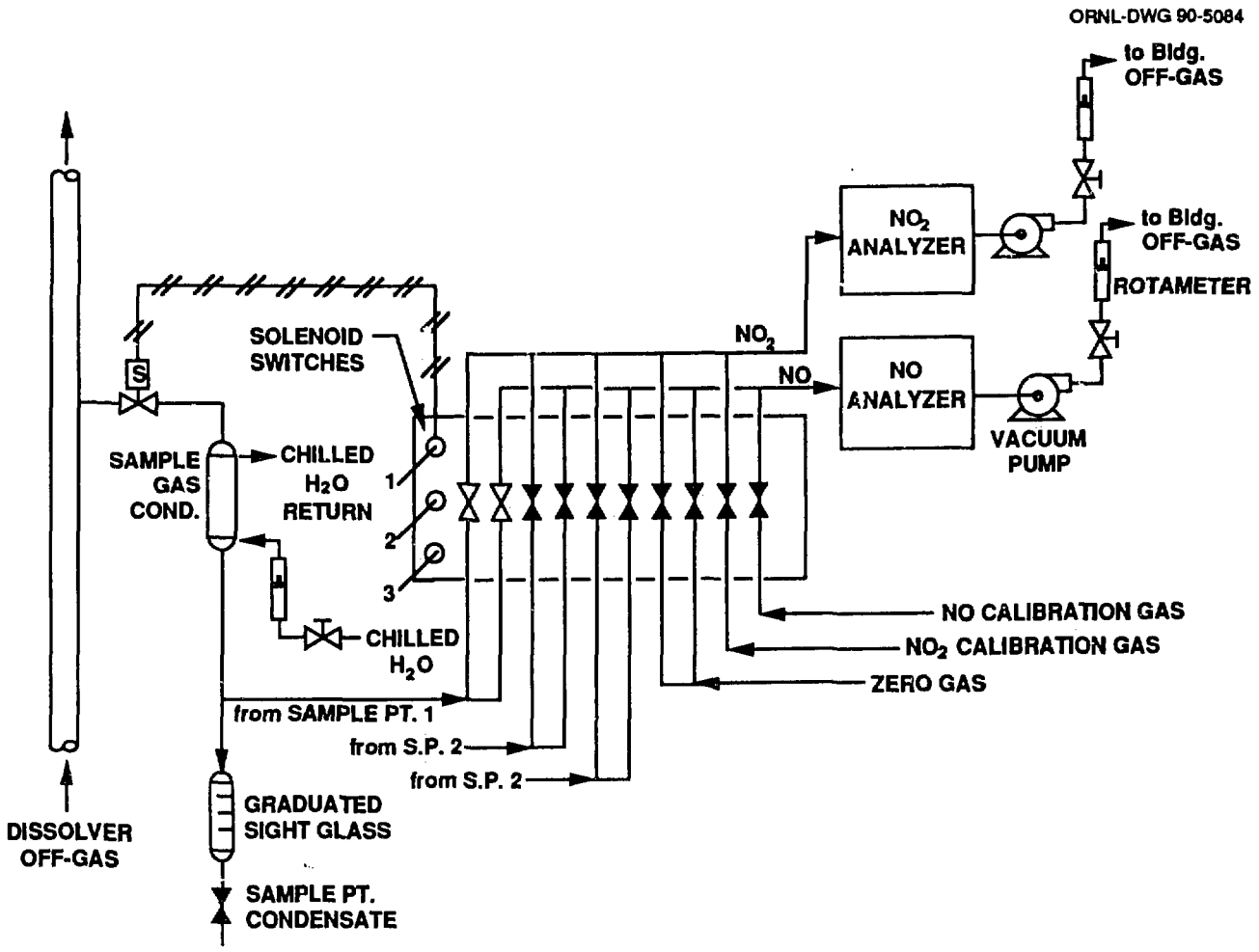

Fig. 4. Analyzer station *A* schematic.

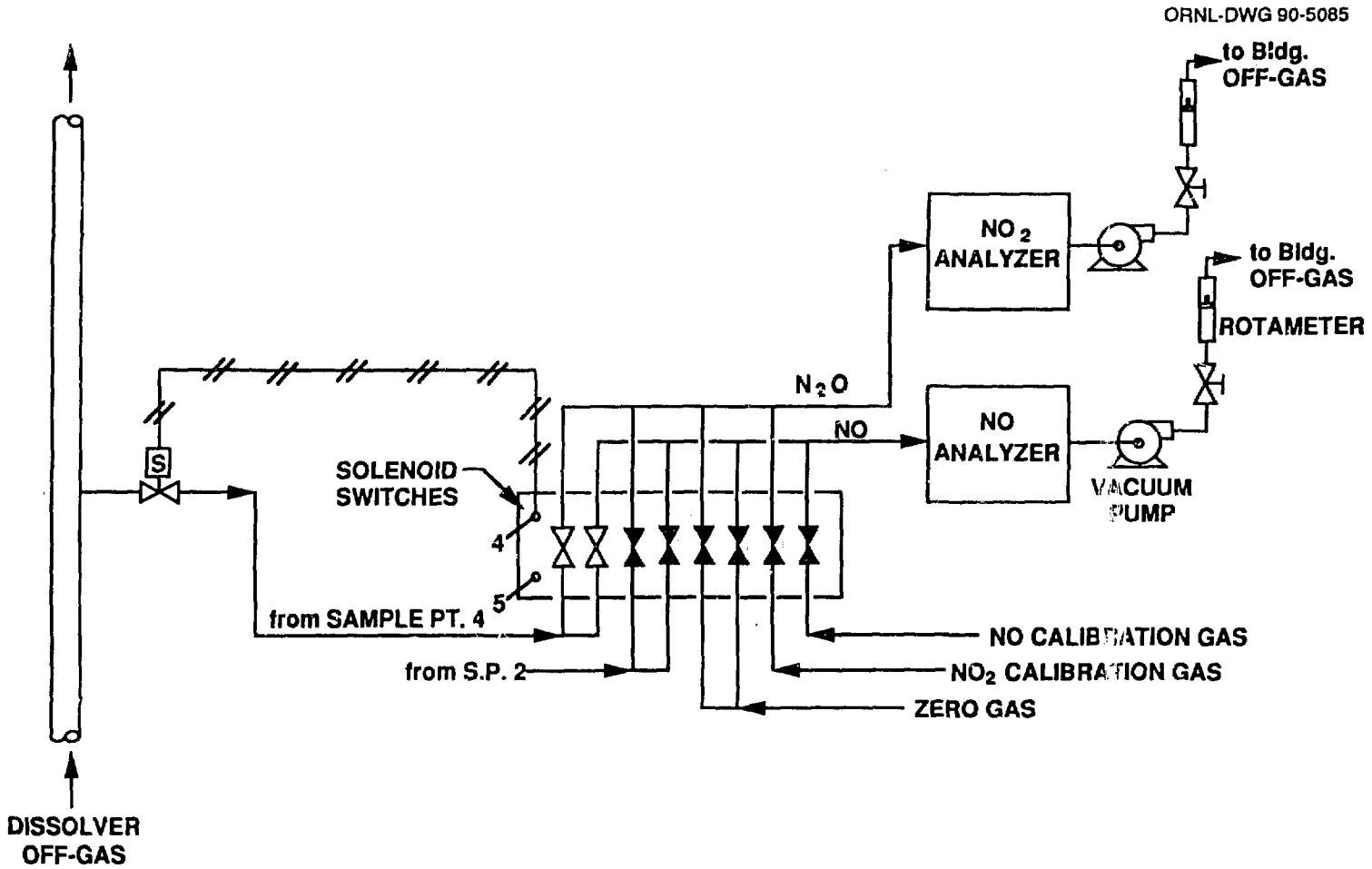

Fig. 5. Analyzer station *B* schematic.

3.2 Phase 4

Phase 4 testing was performed in two parts. In part A, additional data were obtained regarding the behavior of NO_x in the system. Based on the results of the Phase 3 tests, a range of DOG NO and NO_2 concentrations were selected for use in Phase 4. To minimize the likelihood of process upsets and to increase the manpower availability for sampling, uranium dissolution was not performed during this phase. Instead, NO and NO_2 from commercially available gas bottles were used to simulate dissolver vapor-phase effluents.

The NO_x analyzer stations were configured as in Phase 3. In addition to the liquid samples collected in Phase 3, samples of the dissolver product stream were taken from both the digesters and the dissolver seal pot (which is located in the product solution line immediately downstream of the dissolver). To study the effect of gas flow rate on DOG system performance, an air addition line was installed at the acid-feed end of the dissolver. The flow through this line was controlled and metered by means of a rotameter/needle valve combination.

In part B of Phase 4 testing, iodine was added to the dissolver in an aqueous 0.2 M KI, 0.4 M $NaNO_2$ solution. The solution also contained approximately 1.5 mCi of 131-I, which was used as a tracer. Gas-phase iodine samples were collected by adsorption onto activated carbon beds using the sampler configuration shown in Fig. 6. As the figure indicates, each sampler consisted of two adsorption beds in series (to ensure complete adsorption); a rotameter to measure sample gas flow; a vacuum pump to induce flow through the adsorption beds; and an ice bath to dry the sample gas, protecting the vacuum pumps from condensate. Samples were taken at locations corresponding to the NO_x gas sample locations. In addition, iodine gas sampling was performed downstream of the IODOX column. Because of the extremely corrosive nature of iodine in the form HI, the NO_x analyzers were valved out of the off-gas system during this last phase of testing.

During Phase 4, the IODOX system was operated to remove iodine from the NO_x scrubber effluent gas stream. The acid concentration system was also operated in conjunction with IODOX in order to generate the hyperazeotropic acid required for iodine scrubbing.

During Phase 4B, liquid samples were collected from the overhead condensers, the dissolver seal pots (dissolver product stream), the dissolver KI feed solution, the digesters, the NO_x scrubber bottoms tank, the acid concentrator, the iodine concentrator in the IODOX system, and the acid product surge tank in the acid concentration system.

Analyses for iodine content of gas samples and liquid samples were performed by measuring the gamma activity level of

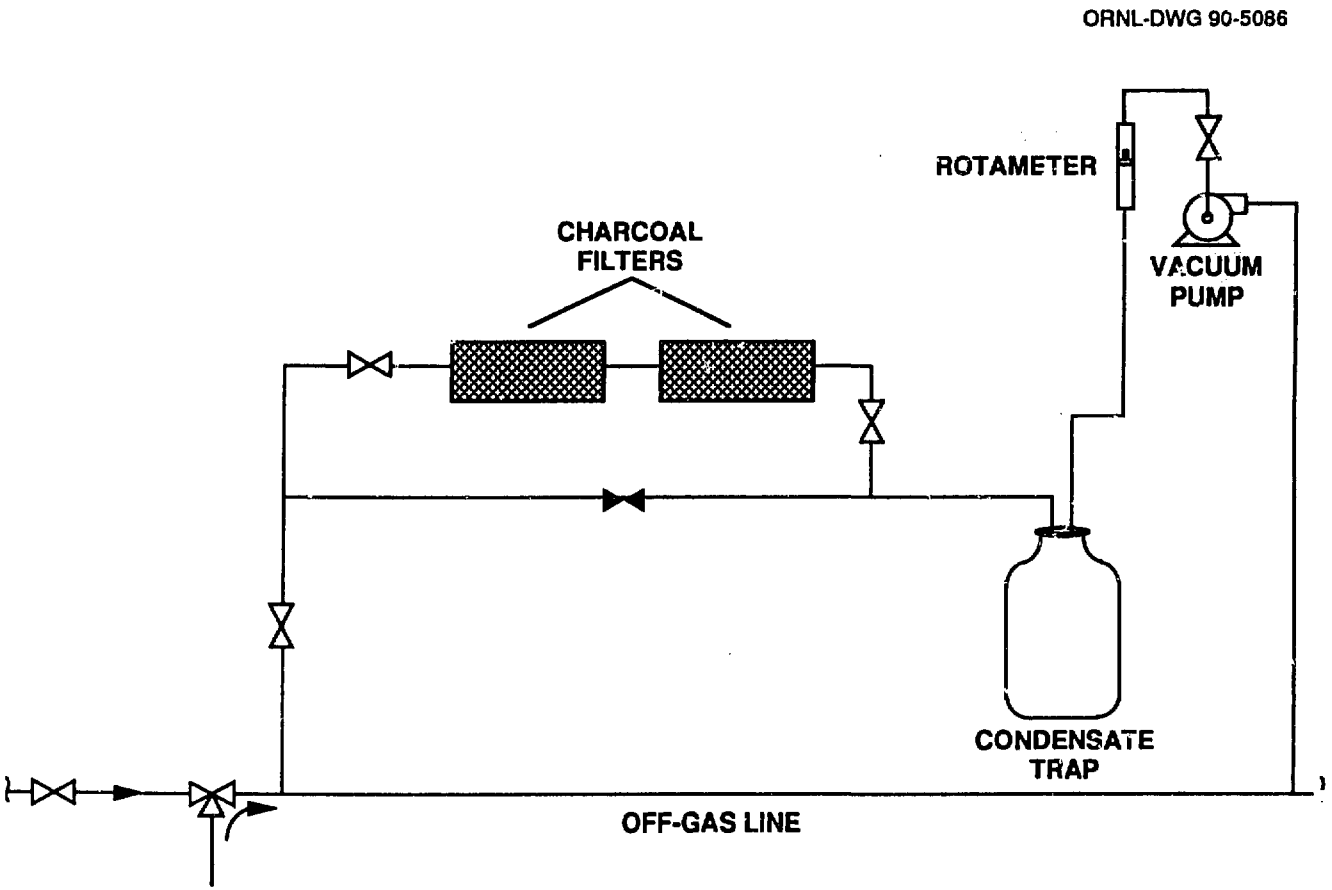

Fig. 6. Vapor-phase iodine sampling system.

the samples. By using the known concentration of the dissolver KI feed solution and the sample volume, the concentration/gamma activity ratio was determined. Similarly, vapor phase iodine concentrations were derived from the observed gamma activity level, the flow rate of sample gas through the adsorption beds, and the duration of flow. In addition to iodine, all liquid samples collected were also analyzed for HNO_2 and HNO_3 content. Liquid-phase iodine samples were analyzed by wet chemical techniques in addition to the gamma activity method.

4. Results

4.1 Phase 3

The results from Phase 3 were somewhat sporadic, because of operational difficulties with both the dissolver and the feed mechanism. These difficulties resulted in test termination after 15 h of data collection; hence, steady state with respect to HNO_2 and HNO_3 liquid-phase concentrations was not achieved in the DOG scrubbing system. However, the vapor-phase results indicate that at a feed rate of 500 kg U/day and over the range of DOG flows from 500 to 1000 SLM (dry gas basis), the NO concentration in the off-gas exiting the dissolver ranged from near zero to 0.1%, and that of NO_2 ranged from 0.5 to 1.25% (Fig. 7).

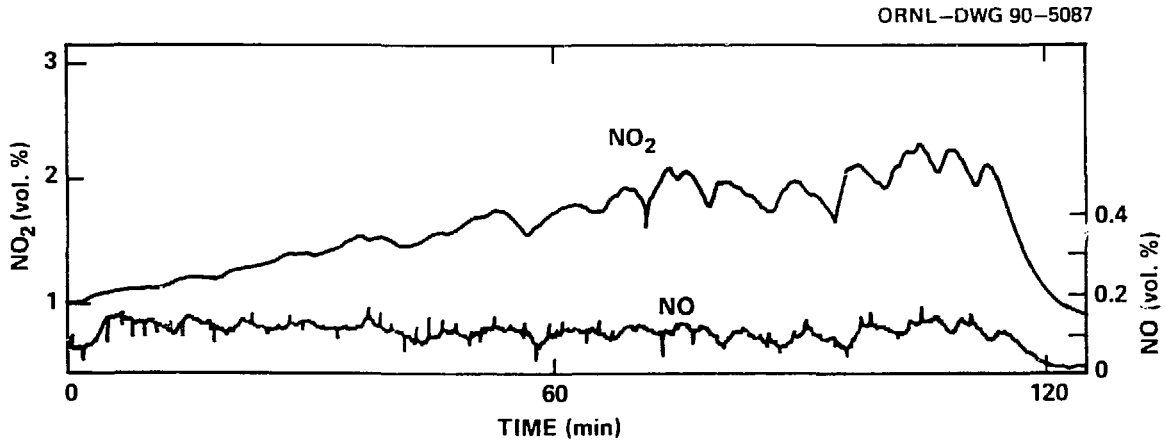

Fig. 7. NO, NO_2 concentrations at the dissolver outlet (Sample Point 1).

NO_2 concentrations recorded at the dissolver exit were observed to increase steadily during a uranium oxide feed period. NO concentrations observed at this point were relatively stable throughout a simulated shear cycle. In contrast, the concentrations of both NO and NO_2 at Sample Points 2, 3, and 4 were observed to rise and fall sharply during a shear cycle, at a frequency corresponding to that of uranium oxide addition. A possible explanation for this observation involves the accumulation of liquid in the sample line between Sample Point 1 and the NO_x analyzers. Because of the relatively high humidity of the off-gas stream exiting the dissolver and the relatively short residence time of the gas in the sample condenser, it is expected that condensate accumulates in this line during testing. This supposition is supported by the surprisingly small amounts of condensate recovered from the Sample Point 1 condenser.

The consistent shift in the concentrations of NO and NO_2 between Sample Points 1 and 2 (Fig. 8) can only be explained by the occurrence of chemical reactions between the dissolver and first condenser. Vapor-phase chemical reactions that may occur in the NO_x-H_2O-HNO_3 system include:[2]

$$2NO_2\ (g) \leftrightarrow N_2O_4\ (g)\ , \tag{2}$$

$$NO\ (g) + NO_2\ (g) \leftrightarrow N_2O_3\ (g)\ , \tag{3}$$

$$NO\ (g) + NO_2\ (g) + H_2O\ (g) \leftrightarrow 2HNO_2\ (g)\ , \tag{4}$$

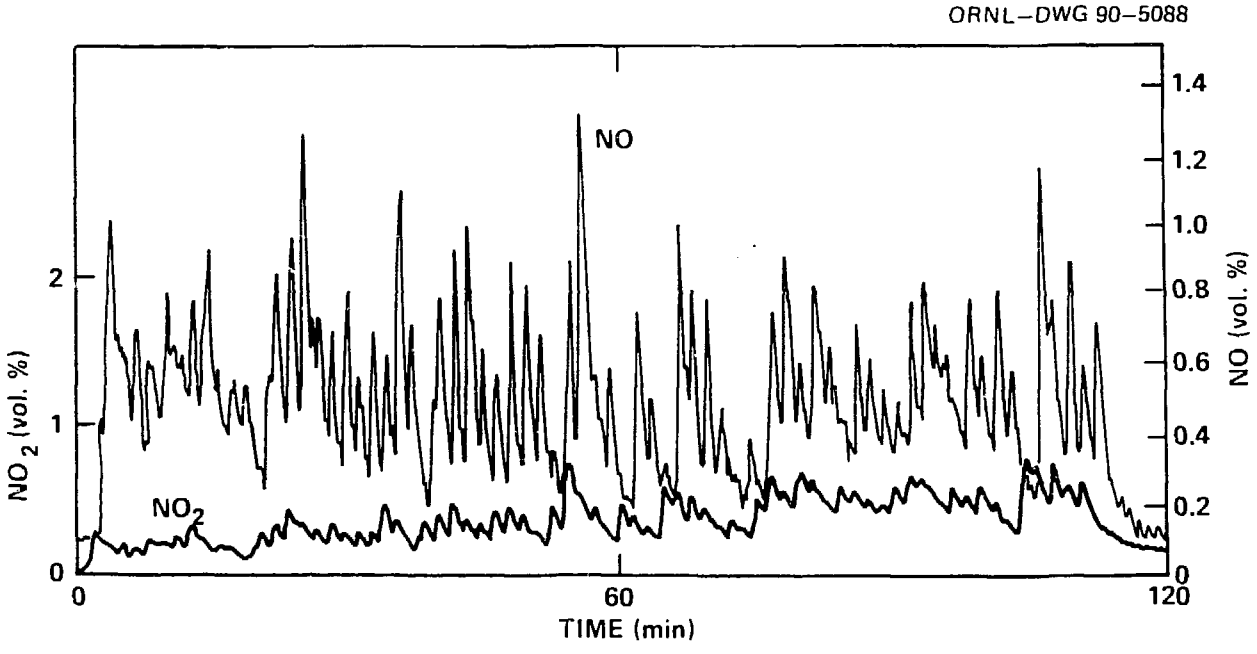

Fig. 8. NO, NO_2 concentrations at first condenser inlet (Sample Point 2).

$$3NO_2\ (g) + H_2O\ (g) \text{ <--> } 2HNO_3\ (g) + NO\ (g)\ , \qquad (5)$$

and

$$2NO\ (g) + O_2\ (g) \text{ --> } 2NO_2\ (g)\ . \qquad (6)$$

A proposed stoichiometry for the dissolution reaction of U_3O_8 (the uranium oxide form used during Phase 3) is

$$U_3O_8 + 7.35HNO_3 \text{ --> } 3UO_2(NO_3)_2 + NO_2 + 0.35NO + 3.65H_2O\ . \qquad (7)$$

The failure to develop a homogenous off-gas mixture in the dissolver coupled with the probable occurrence of chemical reactions involving NO, NO_2, and H_2O prevents the verification of this equation from the data collected in Phase 3.

Equilibrium constants calculated for reactions (2), (3), and (4) at the nominal dissolver off-gas temperature of 363 K are 0.116 atm^{-1}, 0.031 atm^{-1}, and 0.084 atm^{-2} respectively. Given the typical concentrations of NO and NO_2 in the dissolver off-gas are on the order of 10^{-2} atm, the concentrations of HNO_2, N_2O_4, and N_2O_3 inside the dissolver will be negligible, regardless of rate.

In addition to the gas samples, condensate from the off-gas was collected at each of the first three sample points. The HNO_3 concentration in these samples ranged from 1.2 to 1.54 M at Sample Point 1, from 0.33 to 0.74 M at Sample Point 2, and 1.68 to 1.7 M at Sample Point 3.

To determine the minimum relative humidity of the off-gas at Sample Point 2, an off-gas flow rate at the upper end of the observed range (1000 SLM dry air) is selected. Assuming the air exiting the second condenser is saturated with water at 293 K, the relative humidity of the gas entering the first condenser was determined by measuring the rate of condensate removal at each of the two condensers. During Phase 3 testing, these condensate rates were observed to be 150 ml/min at the first condenser and 70 ml/min at the second condenser, nominally. Therefore, the off-gas entering the first condenser must have contained approximately 240 g of water in approximately 1300 g of dry air, and has a relative humidity at 343 K (the nominal gas temperature at the first condenser inlet) of 75%.

Studies by Smith[3] indicated that the formation of NO_2 from NO and HNO_3 by reverse reaction (5) is apparently catalyzed by NO_2 and H_2O. Studies by Leffers[4] et al. using a wetted wall column contacted NO with aqueous HNO_3. These studies determined that NO is oxidized to NO_2 by vapor-phase nitric acid and then is absorbed into the liquid phase after conversion to N_2O_4.

Given that the presence of a significant amount of HNO_3 in the dissolver off-gas is indicated by the concentration measured in the condensate Sample Point 1, and that a considerable

quantity of water vapor is also present, it appears likely that reaction (5) occurs in the reverse direction. This is especially true at the dissolver outlet where the concentrations of water and nitric acid vapor are at the highest levels in the DOG system. The occurrence of this reaction would account for the deviation between the observed ratio of NO to NO_2 at the dissolver and the stoichiometric ratio indicated by reaction (7). The oxidation of NO to NO_2 by reaction (6) may also be partly responsible the overabundance of NO_2 at the dissolver outlet, although data from a number of researchers indicate that this reaction will occur at a rate one order of magnitude slower than reverse reaction (5).

The depletion of NO_2 and the accompanying increase in NO concentration between Sample Points 1 and 2 are most likely due to the occurrence of reaction (2) in the vapor phase, followed by the equilibrium absorption of NO_2-N_2O_4 according to the expression

$$1.5N_2O_4\ (g) + H_2O\ (l) \leftrightarrow 2HNO_3\ (l) + NO\ (g)\ , \qquad (8)$$

which has been proposed by Carberry.[5] This reaction is facilitated by the condensation of water inside the uninsulated off-gas pipe in the 40 ft section between Sample Points 1 and 2. Additional depletion of NO_2 and formation of NO is probably because of the occurrence of the liquid phase reaction

$$N_2O_4\ (l) + H_2O\ (l) \rightarrow HNO_3\ (l) + HNO_2\ (l)\ , \qquad (9)$$

and the subsequent decomposition of HNO_2 according the expression

$$3HNO_2\ (l) \leftrightarrow HNO_3\ (l) + H_2O\ (l) + NO\ (g)\ . \qquad (10)$$

The occurrence of reaction (10) in Phase 3 testing is indicated by the low concentrations of HNO_2 observed in the liquid phase throughout the off-gas system.

The concentrations of NO in the gas phase immediately upstream of the second condenser (Sample Point 3) were slightly lower than concentrations measured immediately upstream of the first condenser. However, the time-averaged concentrations of NO_2 at Sample Point 3 during two shear cycles were 1.3 and 1.7% (Fig. 9), which are significantly higher than the average of 0.4% measured at Sample Point 2 during two previous cycles. The only apparent mechanism for NO_2 formation without significant changes in the concentration of NO is the decomposition of nitrous acid by reaction (10) followed by oxidation of all NO formed. In fact, the HNO_2 concentration in the condensate samples decreases from Sample Point 2 to Sample Point 3 (from 2.0 to 0.2 mg/ml) while the HNO_3 concentration increases. At the conditions of the off-gas exiting the first condenser, the rate of NO oxidation is .00475 atm/s. At this relatively slow rate, complete conversion of the NO formed by HNO_2 decomposition between Sample Points 2 and 3 is improbable.

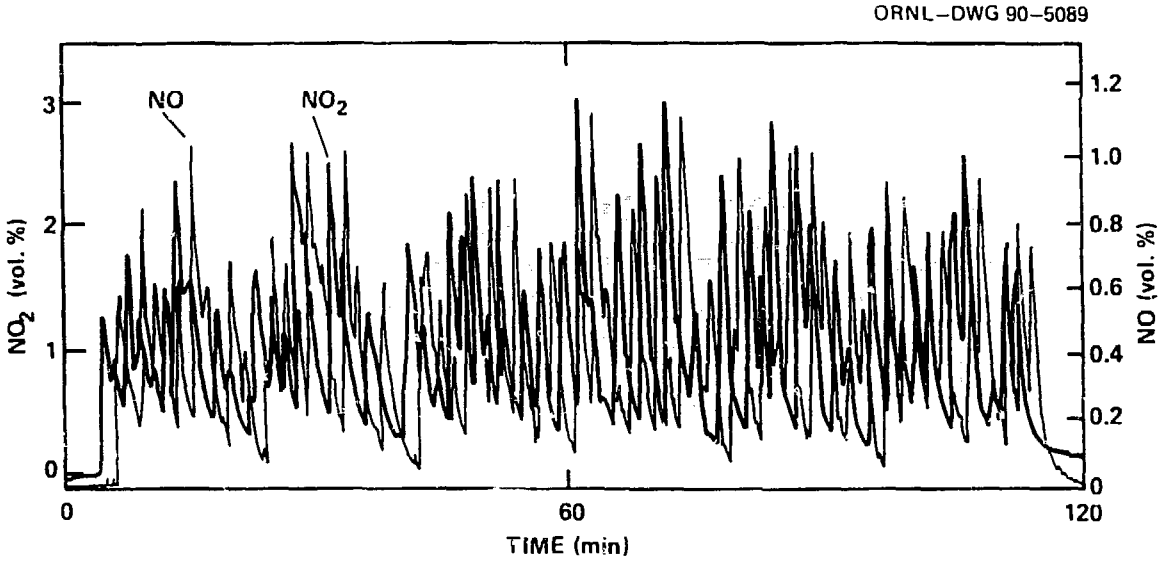

Fig. 9. NO, NO_2 concentrations at second condenser inlet (Sample Point 3).

The off-gas pulses evident at Sample Points 2 and 3 were also observed downstream of the second condenser (Sample Point 4). At this location, the measured concentrations of NO and NO_2 ranged from 1.0 to 1.1% and 0.3 to 0.5% respectively (Fig. 10). The increase in NO and decrease in NO_2 concentration are most likely due to the occurrence of reactions (2), (8), (9), and (10). Reactions (8) and (9) are enhanced between Sample Points 3 and 4 by the condensation of most of the water remaining in the vapor phase downstream of the first condenser. The increase in the HNO_2 concentration in the condensate from the second condenser supports this hypothesis.

The NO and NO_2 concentration spikes seen at Sample Points 2, 3, and 4 disappear at Sample Point 5, located at the exit of the NO_x scrubber. This is most likely due to the gas residence time within this vessel. NO concentrations at the scrubber outlet ranged from 0.2 to 0.4%. NO_2 concentrations ranged from 0.2% to a level not detectible by the infrared analyzer used (Fig. 11). These results are as expected and reflect the absorption of NO_2 into water by reactions (8) and (9). The depletion of NO_2 by absorption then drives reaction (6) toward the oxidation of NO, resulting in the depletion of the oxide.

4.2 Phase 4

NO_x-H_2O-HNO_x System Behavior. The somewhat artificial conditions imposed influenced the results of the NO_x portion of Phase 4 testing which, as a consequence, are not directly representative of off-gas behavior during fuel dissolution. As stated previously, both NO and NO_2 were fed into the dissolver

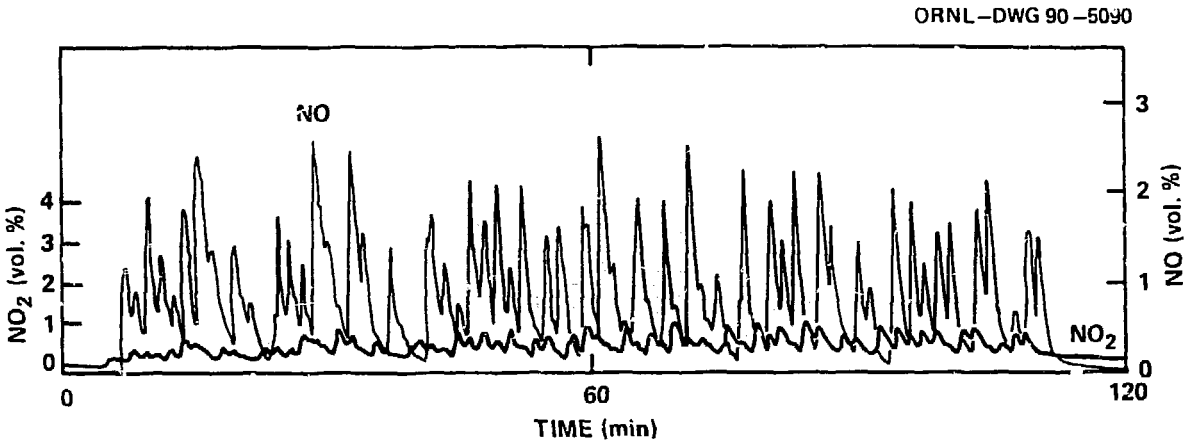

Fig. 10. NO, NO_2 concentrations at second condenser outlet (Sample Point 4).

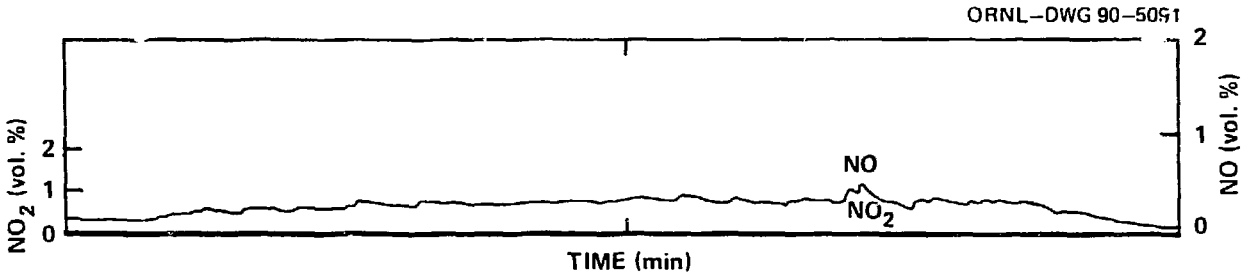

Fig. 11. NO, NO_2 concentrations at NO_x scrubber outlet (Sample Point 5).

from gas cylinders on a continuous flow basis during Phase 4 testing. Both the NO and NO_2 flows into the dissolver were metered to generate NO and NO_2 concentrations in the dissolver off-gas over the range of 1 to 2.5% for each component. The concentrations of the components relative to one another were not adjusted in any way to simulate the U_3O_8 dissolution stoichiometry described in reaction (7). Recognizing that these conditions limit the direct applicability of Phase 4 NO_x results to dissolver off-gas behavior, the elimination of the fluctuations introduced by the intermittent nature of normal dissolver feeding simplifies analysis of interacting NO_x-H_2O-HNO_3 reaction mechanisms.

The amount of NO charged to the dissolver (Table 1) was approximately six times the quantity measured in the off-gas at

Table 1. Dissolver inputs

Sample set	NO_2 feed SLM	NO feed SLM	DOG LPM	DOG K	Material Balance DOG $\%NO_2$	Material Balance DOG %NO
1	0	0	a	a	a	a
2	6.32	8.68	a	a	a	a
3	0	0	a	a	a	a
4	8.60	12.47	1006	348.6	1.02	1.48
5	9.00	12.87	817	351.0	1.32	1.89
6	8.57	8.97	1019	352.3	1.01	1.06
7	11.36	0	744	353.0	1.84	0
8	9.12	15.48	a	a	a	a
9	0	0	686	352.0	0	0
10	10.64	21.82	591	353.1	2.17	4.45
11	8.09	8.89	858	348.0	1.12	1.23
12	8.64	13.34	1008	346.9	1.01	1.57
13	8.58	11.39	1102	346.5	0.92	1.22
14	8.58	15.26	943	346.6	1.08	1.91
15	8.44	11.55	964	344.7	1.03	1.41
16	4.41	17.79	1077	346.8	0.48	1.96
17	9.02	17.93	804	346.1	1.32	2.63
18	11.86	18.16	1185	346.8	1.18	1.81
19	12.06	18.48	998	346.8	1.43	2.19
20	11.47	19.02	803	352.1	1.72	2.85
21	a	0	866	352.0	a	0
22	11.64	0	707	351.2	1.97	0
23	5.28	7.23	859	362.5	0.76	1.04
24	5.29	7.38	945	371.2	0.71	0.99
25	0	6.76	960	364.5	0	0.97
26	0	7.17	842	355.2	0	1.03
27	0	23.27	1013	344.8	0	2.70
28	0	0	1142	363.7	0	0
29	0	19.61	1151	343.2	0	0
30	0	23.83	1041	340.1	0	2.66

[a] No data recorded.

the dissolver off-gas outlet (Table 2). NO_2 results are somewhat inconsistent, with increases in the dissolver NO_2 effluent over the amount charged occurring in approximately half the sample sets collected. As in Phase 3, significant quantities of water and nitric acid were found at the dissolver vapor outlet. These conditions are conducive to the occurrence of reverse reaction (5), in which NO is depleted and NO_2 formed. Under conditions of low NO feed gas flow into the dissolver, the amount of NO_2 exiting the dissolver was found to be equal to or slightly less than the inlet amount. However, at higher inlet NO feed rates, the effluent NO_2 concentration was always higher than would be expected on the basis of the NO_2 feed rate. These findings also support the occurrence of reverse reaction (5) in the dissolver.

Table 2. Sample Point 1 Data

Sample set	Analyzer %NO	Analyzer %NO_2	Temp. (K)	Condensate rate (ml/min)	HNO_2(l) (M)	HNO_3(l) (M)
6	0.15	0.75	352.3	0	[a]	[a]
9	0.15	0.69	352.0	0.0083	2.6E-7	2.32
10	0.15	0.69	353.1	0.0083	7.4E-7	2.94
13	0.00	0.20	346.5	0	[a]	[a]
14	0.30	1.10	346.6	0	[a]	[a]
16	0.12	0.94	346.8	0.558	5.7E-7	2.64
19	0.16	0.87	346.8	0.667	4.3E-7	2.51
22	0.15	0.20	351.2	0	[a]	[a]

[a]No data available.

As in Phase 3, a shift in NO concentration between Sample Points 1 and 2 was observed, with the NO level increasing by from 30 to 100% (Table 3). However, in contrast to the results in Phase 3, a slight increase in NO_2 concentration between Sample Points 1 and 2 was also indicated. HNO_3 concentrations in condensate collected at Sample Point 2 are significantly lower than at Sample Point 1. HNO_2 concentrations in the condensate at Sample Point 2 were generally an order of magnitude greater than at Sample Point 1.

The water content of the gas at Sample Point 2 is still considerable, based on the rate of condensation in the first overhead condenser (Table 4). However, it is suspected that an undetermined amount of water present in the gas at Sample Point 1 condenses before reaching Sample Point 2, because of convective cooling of the off-gas piping between the two points. In addition to water removal, this cooling results in the removal of HNO_3 from the vapor phase, explaining the concentration drop seen between the condensates at Sample Points 1 and 2. The presence

Table 3. Sample Point 2 Data

Sample set	Analyzer %NO	Analyzer $\%NO_2$	Temp. (K)	Condensate rate (ml/min)	HNO_2(l) (M)	HNO_3(l) (M)
4	0.33	0.99	354.8	0.167	1.0E-6	0.69
7	0.45	1.36	354.7	0.080	1.0E-2	0.95
11	0.23	0.70	348.7	0.233	8.3E-7	1.59
14	0.32	1.18	345.4	0.150	1.1E-7	1.15
17	0.57	1.14	346.8	0.250	2.0E-7	0.90
20	0.64	0.57	353.2	0.322	1.1E-6	1.38

Table 4. Condenser Data

	First Condenser			Second Condenser		
Sample set	Condensate rate (ml/min)	HNO_2(l) (M)	HNO_3(l) (M)	Condensate rate (ml/min)	HNO_2(l) (M)	HNO_3(l) (M)
1	a	a	a	a	a	a
2	a	5.3E-3	0.31	219.96	a	a
3	a	3.3E-3	0.21	a	1.6E-2	0.83
4	329.94	6.7E-3	0.26	71.49	2.0E-2	1.51
5	208.96	a	a	60.49	1.0E-2	1.61
6	274.95	5.2E-3	0.15	65.99	1.2E-2	0.99
7	142.97	7.8E-3	0.32	76.99	2.7E-2	2.29
8	219.96	9.6E-3	0.64	71.49	6.5E-7	2.76
9	120.98	5.9E-3	0.27	43.99	3.5E-3	2.68
10	76.99	1.4E-2	0.96	27.50	5.8E-2	3.34
11	115.48	3.7E-3	0.32	49.49	1.3E-2	1.38
12	197.96	3.5E-3	0.25	87.98	1.4E-2	1.40
13	197.96	3.9E-3	0.28	87.98	1.9E-2	1.19
14	131.98	4.6E-3	0.31	93.48	5.4E-3	1.36
15	142.97	3.9E-3	0.26	82.49	1.5E-2	1.13
16	219.96	2.8E-3	0.56	93.48	3.7E-2	2.38
17	197.96	3.5E-3	0.58	71.49	2.4E-2	2.96
18	263.95	8.9E-3	0.68	87.98	2.8E-2	2.70
19	153.97	1.4E-6	0.72	87.98	3.3E-2	2.42
20	219.96	1.4E-2	0.92	60.49	3.4E-2	3.20
21	219.96	1.2E-2	0.74	60.49	2.9E-2	2.90
22	126.48	9.1E-3	0.46	27.50	3.0E-2	1.96
23	197.96	a	a	65.99	a	a
24	241.96	5.2E-3	0.25	65.99	1.8E-2	1.45
25	153.97	2.2E-3	0.15	54.99	1.6E-2	0.85
26	197.96	2.4E-3	0.13	54.99	1.2E-2	0.76
27	170.47	1.5E-6	0.27	54.99	3.9E-3	1.50
28	208.96	2.0E-7	0.05	52.24	4.6E-3	0.26
29	258.45	5.7E-3	0.19	54.99	2.0E-2	1.22
30	203.46	7.0E-3	0.26	62.32	2.4E-2	1.51

[a]No data available.

of condensate in the off-gas line allows the absorption of N_2O_4 into H_2O by the two-phase reaction (8), and to a lesser extent by liquid-phase reaction (9). NO is formed directly in reaction (8), and indirectly by the nitrous acid decomposition reaction (10), which follows reaction (9) in series.

Increases in both NO and NO_2 concentrations were indicated at Sample Point 3 (Table 5). However, these increases in concentration are more than offset by decreases in the volumetric gas flow rate from condensation of water, such that the actual quantities of NO and NO_2 in the vapor have now decreased. Increases in the concentrations of HNO_2 and HNO_3 in the off-gas condensate were also observed. These results indicate the absorption of NO, NO_2, and N_2O_4 to form nitric and nitrous acids by the forward reactions (4) and (5). The slight decrease in NO concentration is the result of reaction (6), which is driven by the depletion of NO_2 by absorption. Formation of HNO_2 and HNO_3 by reactions (8), (9), and (10) is also likely. These reactions should occur primarily at the condenser tube surface, as water present in the off-gas at the dissolver outlet is removed before the gas reaches Sample Point 3. Concentrations of HNO_2 and HNO_3 in the condensate from the first condenser range from 0.0024 to 0.0137 M and from 0.15 to 0.96 M respectively (see Table 4).

Table 5. Sample Point 3 Data

Sample set	Analyzer %NO	Analyzer $\%NO_2$	Temp. (K)	Condensate rate (ml/min)	HNO_2(l) (M)	HNO_3(l) (M)
5	0.15	0.80	332.7	0	[a]	[a]
8	0.37	1.48	333.8	0.067	[a]	[a]
12	0.90	1.35	332.2	0.091	3.0E-7	1.35
15	0.38	0.67	333.2	0.150	1.1E-7	1.44
18	0.48	1.03	333.3	0.450	4.1E-7	2.36

[a]No data available.

There is considerable variation between relative NO concentrations recorded at Sample Point 4 (Table 6) and those measured at Sample Point 3. No distinct trend is discernable.

Table 6. Sample Point 4 Data

Sample set	%NO	$\%NO_2$	Temp. (K)
5	0.48	0.42	294.3
7	0.55	0.70	293.7
11	0.33	0.58	297.6
13	0.30	0.37	298.1
15	0.25	0.25	297.7
17	0.55	0.58	294.0
19	0.51	0.53	297.4
21	0.50	0.65	293.7

However, all recorded NO_2 measurements at Sample Point 4 indicate a significant decrease in concentration from Sample Point 3. Significant increases in the HNO_2 (from 0.0035 to 0.0585 M) and HNO_3 (from 0.76 to 3.34 M) concentrations in the condensate from the second condenser were observed (see Table 4). These results point toward occurrence of NO_2 and N_2O_4 depletion by absorption. It is likely that some of the removal is due to the gas phase reactions (4) and (5). However, given the large quantity of water removed from the off-gas in the first condenser, it is more likely that the decrease in NO_2 concentration is the result of wetted-wall-effect absorption inside the condenser tubes by reactions (8) and (9).

Significant decreases in the quantities of NO and NO_2 present were observed at Sample Point 5, the DOG scrubber vapor outlet (Table 7). The reductions in NO concentration are

Table 7. Sample Point 5 Data

Sample set	%NO	$\%NO_2$	Temp. (K)
4	0.23	0	293.8
6	0.18	0	292.4
8	0.25	0.15	294.2
10	0.02	0.27	294.2
12	0.33	0.30	294.2
14	0.18	0.28	293.6
16	0.23	0	294.1
18	0	0.33	294.1
20	0.18	0	293.8
22	0.15	0	294.0

somewhat inconsistent, ranging from nearly 50% to nearly zero. The data seem to indicate a correlation between higher NO removal efficiencies and higher concentrations of NO_2 in the scrubber effluent gas. This finding indicates the occurrence of NO oxidation according to reaction (6). The large decrease in NO_2 concentration coupled with a consistent upward trend in nitric acid concentration in the recirculated scrubber solution is the result of NO_2 absorption. The favored mechanisms for absorption are reaction (8), which occurs in conjunction with the N_2O_4-NO_2 equilibrium relationship, and reaction (9), because of the relatively low operating temperature of the scrubber (293 K). A lack of accumulation of nitrous acid in the scrubbing solution is evidence of the decomposition of the acid by reaction (10).

Unfortunately, continuous recording of the NO and NO_x readings from the infrared analyzers was not performed during Phase 4. Therefore, the damping observed at Sample Point 1 in Phase 3 cannot be verified.

Iodine Behavior. Iodine samples, both those analyzed by gamma activity levels and by wet chemical techniques, were analyzed for total iodine. Therefore, no observations regarding the presence of specific iodine hydrolysis products can be derived. Note also that the condensates collected at Sample Points 1, 2, and 3 during NO_2 sampling were the result of drying the gas before entry into the infrared NO_x analyzers. Neither the analyzers nor the sample gas condensers were operated during iodine sampling because of potential corrosion problems.

Concentration values for vapor-phase iodine at Sample Point 2 were inconsistent with the values at Sample Points 1 and 3 (Table 8). Specifically, the concentration values at Sample

Table 8. Gas-phase Iodine Concentrations, Sample Points 1 - 3

	Sample Point 1		Sample Point 2		Sample Point 3	
Sample set	Iodine (mol/L)	Gas flow (LPM)	Iodine (mol/L)	Gas flow (LPM)	Iodine (mol/L)	Gas flow (LPM)
23	[a]	971	[a]	937	[a]	576
24	2.31E-6	1060	6379E-8	992	2.81E-6	569
25	3.19E-6	953	1.57E-6	911	3.41E-6	626
26	1.18E-6	934	7.00E-7	911	1.59E-6	561
27	1.52E-6	1104	9.74E-7	1094	2.06E-6	785
28	1.77E-4	1233	1.45E-4	1176	2.34E-4	789
29	2.29E-6	1241	1.03E-7	1251	3.69E-6	789
30	2.09E-6	1142	1.25E-6	1163	2.70E-6	787

[a] No data recorded.

Point 2 yield quantities significantly lower than quantities at either Sample Point 1 (upstream) or Sample Point 3 (downstream). Since there is no mechanism for the reappearance of iodine between Sample Points 2 and 3, the boundaries for the front-end iodine balance were established at Sample Points 1 and 3. Gas-phase concentration values at Sample Points 4, 5, and 6 were generally more consistent than data collected at Sample Points 1, 2, and 3 (Table 9).

Table 9. Gas-phase Iodine Concentrations, Sample Points 4 - 6

Sample set	Sample Point 4 Iodine (mol/L)	Sample Point 4 Gas flow (LPM)	Point 5 Iodine (mol/L)	Point 6 Iodine (mol/L)	Gas flow[a] (LPM)
23	b	460	b	b	407
24	2.30E-6	452	1.96E-6	1.47E-6	400
25	2.04E-6	527	1.32E-6	6.51E-7	465
26	9.46E-7	460	9.36E-7	7.94E-7	407
27	1.21E-6	684	1.63E-6	9.89E-7	600
28	1.78E-4	671	1.05E-4	4.10E-5	607
29	1.91E-6	687	1.41E-6	1.48E-6	603
30	1.54E-6	675	1.43E-6	1.27E-6	592

[a] Flow rates were approximately equal at Points 5 and 6.
[b] No data recorded.

Material balances performed across the first condenser typically close within 20%. Lack of closure is most likely from inconsistencies in the collection of gas samples. More importantly, the analysis of condensate from the first condenser, both by chemical and radiological techniques, detected little or no iodine in 5 of 7 samples (Table 10). In the other two sample

Table 10. Liquid-phase Iodine Concentrations in the DOG system

Sample set	First condenser I (mol/L)	Second condenser I (mol/L)	Scrubber bottoms tank I (mol/L)	Acid concentrator I (mol/L)
23	a	a	a	a
24	0	6.70E-4	3.31E-4	0
25	0	2.76E-4	0	0
26	0	1.97E-4	9.46E-5	0
27	0	1.18E-4	0	1.18E-4
28	1.58E-4	1.58E-4	0	1.18E-4
29	0	1.97E-4	0	2.36E-4
30	3.94E-5	1.18E-4	0	1.97E-4

[a] No data recorded.

sets, the amounts of iodine recycled to the dissolver in the liquid from the first condenser were 0.015 and 0.337% of the input iodine.

Material balances around the second condenser generally accounted for only 60% of the input iodine. However, the concentrations of iodine in the condensate from this condenser were consistently on the order of 10^{-4} mol I/min. At the nominal 55 ml/min condensation rate observed during this Phase of testing (Phase 4), the percentage of iodine removed from the vapor stream in the second condenser ranged from 0.31 to 1.80%.

Samples from the NO_x scrubbing system indicate that approximately 2% of the iodine fed to the dissolver was returned in the acid recycle stream (see Table 10). Inexplicably, the concentrations of iodine in the acid concentrator tank were higher than those in the scrubber bottoms tank in about half of the sample sets.

Observed liquid-vapor distribution coefficients for iodine at the first condenser were typically near zero. Distribution coefficients at the second condenser were typically of the order 10^2. The data from the second condenser correspond closely with distribution coefficients calculated using Eq. (1). The data from the second condenser are also consistent with distribution coefficients determined by the simultaneous solution of the equations

$$[HIO] = (K_{19}[I_2]_{aq})/([H^+][I^-]) \quad , \tag{11}$$

$$[H_2OI^+] = (K_{20}[I_2]_{aq})/([I^-]) \quad , \tag{12}$$

$$[I_3^-] = K_{18}[I_2]_{aq}[I^-], \tag{13}$$

$$[I^-] = ((K_{20}[I_2]_{aq})/(1 + K_{18}[I_2]_{aq}) + (K_{19}[I_2]_{aq})/([H^+](1 + K_{18}[I_2]_{aq})))^{1/2} \quad , \tag{14}$$

$$[I_2]_{aq,TOT} = [I_2]_{aq} + 0.5([HIO] + [H_2OI^+] + [I^-] + 3[I_3^-]) \quad , \tag{15}$$

$$D = [I_2]_{aq,TOT}/[I_2]_g \quad , \tag{16}$$

as given by Parsly.[6] These expressions are derived from the equilibrium relationships for the water-iodine system

$$I_2(g) \text{ <--> } I_2(aq) \quad , \tag{17}$$

$$I_2(aq) + I^- \text{ <--> } I_3^- \quad , \tag{18}$$

$$I_2(aq) + H_2O \text{ <--> } H^+ + I^- + HIO \quad , \tag{19}$$

$$I_2(aq) + H_2O \text{ <--> } H_2OI^+ \; I^- \quad . \tag{20}$$

The liquid-phase concentration of iodine from the first condenser condensate was somewhat lower than predicted by Eq. (1). Given the relatively low concentrations of iodine in both phases, this deviation is not unreasonable.

IODOX System Performance. The results of material balances around the IODOX scrubbing column indicate poor performance in iodine removal. Removal efficiencies ranged from 11 to 61%, with the highest efficiency achieved at the highest inlet iodine concentration. The average removal efficiency over 6 sample sets was 34%. The resultant decontamination factor of 1.5 is several orders of magnitude less than values reported by Groenier.[7] Potential errors in the collection of the gas sample are not likely to have produced such a large deviation. The brevity of the IODOX operation period made it unlikely that steady state was approached. For this reason, and the extreme variation between experimental results reported herein and data obtained in earlier work, the validity of the IODOX results obtained in this study is suspect.

5. Conclusions

Results from the evaluation of NO_x behavior in all phases of testing are consistent with reaction mechanisms previously reported. The most significant findings are the strong interactions among the various chemical species in the NO_x-HNO_x-H_2O system at the relatively low component concentrations present in the dissolver off-gas system.

The results of this study indicate that the extent of incidental NO_x treatment, which occurs in the off-gas condensers, is determined by the composition of the entering gas. However, over the range of feed conditions studied, the combined NO and NO_2 concentration in the effluent from the second condenser never exceeded 1.5%.

The NO_x scrubber was surprisingly efficient, given the low concentrations of NO and NO_2 present in the feed gas stream. However, given the low concentrations of NO and NO_2 present downstream of the off-gas condensers, no further NO_x removal is required to effectively remove iodine.

One limitation in the NO_x study was the ability to simultaneously monitor only one sample point at each of the two anaylzer stations. This severely restricts the ability to perform real-time mass balances across individual sections of the off-gas system.

The results from iodine testing in the DOG system confirmed the results obtained previously by Lewis and Jubin.[1] Negligible amounts of iodine were recycled to the dissolver in the condensate from the first condenser. A minimal amount (2% maximum) of the iodine in the dissolver off-gas was recycled in the condensate from the second condenser. In addition, a 2% recycle of iodine from the NO_x scrubbing system was observed. It may be concluded that, at steady state, the double overhead condenser/NO_x scrubber configuration results in a 4 to 5% recycle of iodine and 99% recycle of the nitric acid and water present in the dissolver off-gas. Removal of the NO_x scrubbing system from the loop reduces the amount of iodine recycle to 2 to 3%.

The iodine removal efficiencies observed in the IODOX system were considerably lower than anticipated. Unfortunately, the short duration of the test produced insufficient data to determine the cause of the poor scrubber performance.

REFERENCES

1. B. E. Lewis and R. T. Jubin, "Demonstration of the Iodine and NO_x Removal Systems in the Oak Ridge National Laboratory Integrated Equipment Test Facility," Proceedings of the 19th DOE/NRC Nuclear Air Cleaning Conference, Seattle, Wash., August 1986.

2. R. M. Counce, The Scrubbing of Gaseous Nitrogen Oxides in Packed Towers, ORNL-5675, Martin Marietta Energy Systems, Oak Ridge Natl. Lab., November 1980.

3. J. H. Smith, J. Am. Chem. Soc., 69, 1742 (1947).

4. J. B. Lefers et al., Chem. Engr. Sci. **35**, 145 (1980).

5. J. Carberry, Chem. Engr. Sci. **9**, 189 (1959).

6. L. F. Parsly, Design Considerations of Reactor Containment Spray Systems-Part IV, Calculation of Iodine - Water Partition Coefficients, ORNL - TM - 2412, Part IV, Martin Marietta Energy Systems, Oak Ridge Natl. Lab., January 1970.

7. W. S. Groenier, An Engineering Evaluation of the IODEX Process: Removal of Iodine from Air Using a Nitric Acid Scrub in a Packed Column, ORNL-TM-4125, Martin Marietta Energy Systems, Oak Ridge Natl. Lab., August 1973.